

Arhodomonas sp. Strain Seminole and Its Genetic Potential To Degrade Aromatic Compounds under High-Salinity Conditions

Sonal Dalvi,^a Carla Nicholson,^a Fares Najar,^c Bruce A. Roe,^c Patricia Canaan,^b Steven D. Hartson,^b Babu Z. Fathepure^a

Department of Microbiology and Molecular Genetics^a and Department of Biochemistry and Molecular Biology,^b Oklahoma State University, Stillwater, Oklahoma, USA; Stephenson Research and Technology Center, University of Oklahoma, Norman, Oklahoma, USA^c

Arhodomonas sp. strain Seminole was isolated from a crude oil-impacted brine soil and shown to degrade benzene, toluene, phenol, 4-hydroxybenzoic acid (4-HBA), protocatechuic acid (PCA), and phenylacetic acid (PAA) as the sole sources of carbon at high salinity. Seminole is a member of the genus *Arhodomonas* in the class *Gammaproteobacteria*, sharing 96% 16S rRNA gene sequence similarity with *Arhodomonas aquaeolei* HA-1. Analysis of the genome predicted a number of catabolic genes for the metabolism of benzene, toluene, 4-HBA, and PAA. The predicted pathways were corroborated by identification of enzymes present in the cytosolic proteomes of cells grown on aromatic compounds using liquid chromatography-mass spectrometry. Genome analysis predicted a cluster of 19 genes necessary for the breakdown of benzene or toluene to acetyl coenzyme A (acetyl-CoA) and pyruvate. Of these, 12 enzymes were identified in the proteome of toluene-grown cells compared to lactate-grown cells. Genomic analysis predicted 11 genes required for 4-HBA degradation to form the tricarboxylic acid (TCA) cycle intermediates. Of these, proteomic analysis of 4-HBA-grown cells identified 6 key enzymes involved in the 4-HBA degradation pathway. Similarly, 15 genes needed for the degradation of PAA to the TCA cycle intermediates were predicted. Of these, 9 enzymes of the PAA degradation pathway were identified only in PAA-grown cells and not in lactate-grown cells. Overall, we were able to reconstruct catabolic steps for the breakdown of a variety of aromatic compounds in an extreme halophile, strain Seminole. Such knowledge is important for understanding the role of *Arhodomonas* spp. in the natural attenuation of hydrocarbon-impacted hypersaline environments.

Hypersaline environments, such as oil fields, industrial effluents, and coastal ecosystems, are often contaminated with high levels of petroleum hydrocarbons (1, 2). Among these, oil and gas production sites pose the greatest risk of soil and groundwater contamination due their large numbers all over the world. They are not only contaminated with a complex mixture of hydrocarbons but also display a wide range of salinities, from very low up to saturated brines. The arid coastlines of Gulf countries are highly saline and susceptible to oil spill and environmental damage. Waste streams from pesticides, chemicals, and pharmaceuticals generate large quantities of highly saline wastewaters (3). Effective bioremediation of such contaminated environments by conventional microorganisms cannot be achieved because salt affects their growth and the bioavailability of hydrocarbons (1, 4). Therefore, halophilic and halotolerant organisms that degrade hydrocarbons have received considerable attention in recent years due to their potential use in the remediation of hydrocarbon-impacted high-salinity environments.

In the last 2 decades, studies have documented the ability of bacteria, archaea, and a few eukaryotes to degrade hydrocarbons under moderate- to high-salinity conditions (5, 6). Among bacteria, members of the genera *Halomonas*, *Marinobacter*, and *Alcanivorax* have been widely reported to degrade aliphatic and aromatic compounds over a broad range of salinities (1, 6–9). The majority of published reports indicate that *Halomonas* spp. are capable of degrading *n*-alkanes, phenolics, and benzoates, but little information exists about their capacity to degrade benzene, toluene, ethylbenzene, and xylenes (BTEX) and polyaromatic hydrocarbons (PAHs). On the other hand, *Marinobacter* and *Alcanivorax* have been reported to degrade mainly aliphatic compounds, BTEX, and PAHs, but not much is known about their

ability to degrade phenols and benzoates under moderate- to high-salt conditions (6).

Among archaea, *Haloferax* (10–13), *Haloarcula* (13, 14), and several members of *Halobacterium* (12, 13, 15) have been shown to degrade both aliphatic and aromatic hydrocarbons in high-salinity environments. Recently Erdoğmuş et al. (16) isolated several archaea, including *Halorubrum* sp. and *Halorubrum ezzemou-lense*, that grew on *p*-hydroxybenzoic acid, naphthalene, phenanthrene, and pyrene as the sole sources of carbon at 20% salinity.

Although these studies provide evidence for degradation of aliphatic and aromatic compounds under high-salt conditions, little is known about genes, enzymes, and metabolic pathways for these compounds. A few recent studies have revealed the presence of genes encoding catechol 1,2-dioxygenase (1,2-CAT), catechol 2,3-dioxygenase (2,3-CAT), and protocatechuate 3,4-dioxygenase (3,4-PCA) enzymes in several strains of phenol- and benzoate-degrading *Halomonas* spp. (17–20). Kim et al. (21) isolated a benzoate- and *p*-hydroxybenzoate-metabolizing halophile, *Chromohalobacter* sp. strain HS-2. Their work showed that benzoate induces the expression of benzoate 1,2-dioxygenase, 1,2-CAT, and 3,4-PCA, while *p*-hydroxybenzoate only induced the expres-

Received 8 May 2014 Accepted 15 August 2014

Published ahead of print 22 August 2014

Editor: R. E. Parales

Address correspondence to Babu Z. Fathepure, babu.fathepure@okstate.edu.

Supplemental material for this article may be found at <http://dx.doi.org/10.1128/AEM.01509-14>.

Copyright © 2014, American Society for Microbiology. All Rights Reserved.

doi:10.1128/AEM.01509-14

sion of *p*-hydroxybenzoate hydroxylase (PobA). Similarly, a few hydrocarbon-degrading archaea belonging to the genera *Haloferax*, *Haloarcula*, *Halobacterium*, and *Halorubrum* have also been shown to possess catabolic enzymes similar to those from nonhalophiles (14, 16, 22). However, in-depth studies are needed to understand the degradation pathways and steps leading to intermediates that enter the tricarboxylic acid (TCA) cycle in organisms that withstand high salinity.

In this article, we report the isolation and metabolic potential of a novel halophile, *Arhodomonas* sp. strain Seminole, from an enrichment culture developed from a crude oil-impacted brine soil. Strain Seminole degrades benzene, toluene, phenol, protocatechuic acid, 4-hydroxybenzoic acid, and phenylacetic acid as the sole sources of carbon and energy. A high-quality draft genome sequence of strain Seminole was used to predict genes involved in the degradation steps of the above aromatic compounds. The predicted pathways were corroborated by semiquantitative identification of enzymes expressed in the cytosolic proteomes of aromatic compound-grown cells using liquid chromatography-tandem mass spectrometry (LC-MS/MS).

MATERIALS AND METHODS

Chemicals and media. Toluene, ethylbenzene, hexadecane, and [¹⁴C]benzene with a specific activity of 33.2 mCi/mol were all purchased from Sigma-Aldrich, MO. The ¹⁴C cocktail used for trapping ¹⁴CO₂ was purchased from R. J Harvey Instrument Corp., NJ. Benzene, three isomers of xylene (*meta*-, *para*-, and *ortho*-xylenes), phenol, and sodium benzoate were purchased from Fisher Scientific, PA. Catechol (CAT), phenylacetic acid (PAA), and 4-hydroxybenzoic acid (4-HBA) were purchased from Alfa Aesar, MA. Gentisic acid (GA) and protocatechuic acid (PCA) were purchased from MP Biomedicals, OH. All other chemicals were of analytical grade and were used without further purification. The composition of mineral salts medium (MSM) used in this study was previously described (23). MSM was supplemented with 2.5 M NaCl and yeast extract (0.01%) for all experiments unless mentioned otherwise. For solidified medium, 1.5% (wt/vol) agar was added prior to autoclaving.

Isolation of strain Seminole. A highly enriched microbial consortium, Sem-2 enrichment (23) capable of completely degrading BTEX within 1 to 2 weeks, was used for the isolation of a benzene-degrading halophilic bacterium. A 10-fold serial dilution of the enrichment was plated onto MSM agar plates supplemented with 1 M NaCl and Luria broth (1/10 total strength) and incubated at 30°C until growth was observed. Individual colonies were tested for their ability to degrade benzene by growing them in 120-ml-capacity serum bottles containing 45 ml of MSM supplemented with 2.5 M NaCl and 2 μl (25 μmol) of neat benzene. Bottles were closed with Teflon-coated septa and aluminum caps. Head-space samples were withdrawn periodically and monitored for consumption of added benzene by gas chromatography (GC) as described previously (23). The culture that showed benzene degradation was selected for further characterization.

16S rRNA gene analysis of strain Seminole. Total genomic DNA of the isolate was extracted using the UltraClean soil DNA kit (MO BIO Laboratories, Inc., CA). To obtain a nearly full-length sequence of the 16S rRNA gene, PCR was performed using two primer sets: 27F [5'-AGAGT TTGATC(A/C)TGGCTCAG-3'] and 1492R [5'-TACGG(C/T)TACCTT GTTACGACTT-3'] (24) and 27F and 1098R (5'-AAGGGTTGCGCTCG TTGCG-3') (25). PCR was performed in a 50-μl reaction mixture as described previously (26). The 16S rRNA gene sequence obtained was compared with sequences in the GenBank nr database using the BLASTN program at NCBI (27). A phylogenetic tree was constructed using the maximum likelihood method in MEGA6 (28).

Ecological distribution of strain Seminole. To screen for *Arhodomonas* sp.-like phylotypes in samples from different locations, specific primer pairs 1465R (5'-GTCTCGACCACACCGTGG-3') and 206F (5'-GTTTC

ATGGTCACGCCGA-3') were designed using the probe design function in the ARB software package (29). The primers were validated by querying them using the probe match function in the Ribosomal database Project (30). Contaminated as well as uncontaminated soil, water, or sediment samples with various levels of salinity were collected from different locations. These include (i) soil from a brine pit at site B, Skiatook, OK, (ii) soil from the Great Salt Plains National Wildlife Refuge, OK, (iii) a water sample from the Dead Sea, Israel, (iv) soil contaminated by a produced water spill from the Tall Grass Prairie Preserve, OK (31), (v) hydrocarbon-impacted saline soil from Kuwait, (vi) soil from an east Texas Chevron site, (vii) sediment and water samples from the base of a mangrove tree in Cabo Rojo, Puerto Rico (32), (viii) soil from a salt-manufacturing plant in Freedom, OK (32), and (ix) wastewater from the Ramat-Hovav Industrial Park, Negev Desert, Israel (33).

DNA extraction, PCR amplification, cloning, and sequencing for the ecological distribution study. Genomic DNA was extracted using an UltraClean soil DNA isolation kit (MO BIO Laboratories, Inc. CA) and FASTDNA spin kit for soil (MP Biomedicals, OH). Genomic DNA was pooled and nested PCR was performed with bacterial primers 27F and 1492R using a protocol described previously (34), followed by *Arhodomonas* sp.-specific primers 206F and 1465R to screen for 16S rRNA genes of *Arhodomonas* spp. PCR was performed in 50-μl reaction mixture that contained 2 μl of the first-reaction PCR product, 1× PCR buffer (Teknova, CA), 2.5 mM MgSO₄, 10 mM deoxynucleoside triphosphate (dNTP) mixture, 1 U of *Taq* DNA polymerase, and 10 μM each forward and reverse primers. PCR with *Arhodomonas* sp.-specific primers was carried out according to the following protocol: initial denaturation at 94°C for 3 min, followed by 30 cycles of denaturation at 94°C for 1 min, annealing at 54°C for 55 s, and elongation at 72°C for 2 min. A final elongation step at 72°C for 8 min was included. All samples were PCR amplified in triplicate. The resulting PCR products of the expected size (approximately 1,250 bp) were gel purified using a QIAquick gel extraction kit (Qiagen, CA). The purified products were then cloned into *Escherichia coli* TOP10 using a TOPO TA cloning kit (Invitrogen, CA) and sequenced at Oklahoma State University Recombinant DNA/Protein Core Facility (Stillwater, OK). The sequences obtained were compared with those in the GenBank nr database using the BLASTN program in NCBI (27). A phylogenetic tree was constructed in MEGA6 to highlight the phylogenetic affiliation of the clones obtained in this study with sequences of closely related *Arhodomonas* spp. in GenBank (28).

Growth and maintenance of strain Seminole. The strain was maintained in 1-liter bottles with 500 ml of MSM supplemented with 2.5 M NaCl and 250 μmol of neat benzene as the sole source of carbon. At the end of 4 weeks, 50% of the content was replaced with fresh MSM containing 2.5 M NaCl, and the pH was adjusted to neutral with 1 N NaOH. This bottle served as the mother culture for all experiments performed in this study.

Degradation of BTEX by strain Seminole. Strain Seminole was grown in 120-ml serum bottles filled with 45 ml of MSM supplemented with 2.5 M NaCl and inoculated with 5 ml of actively growing culture (62 μg biomass protein) from the mother bottle. Bottles were amended with 22 to 25 μmol of neat benzene, toluene, ethylbenzene, or three isomers of xylene (*meta*-, *para*-, and *ortho*-xylene) as the sole sources of carbon and energy. These bottles were closed with Teflon-coated rubber septa and aluminum crimps and incubated in an inverted position at 30°C. Autoclaved control bottles were set up similarly. The BTEX concentrations were monitored periodically by GC as described previously (23). Culture samples (1 ml) were removed periodically for protein estimation by the Lowry method (35). Similarly, microcosms were set up to evaluate the ability of strain Seminole to degrade benzene at different concentrations of NaCl ranging from 0 to 4 M. Mineralization of benzene by the strain was determined by setting up microcosm bottles amended with [¹⁴C]benzene. The production of ¹⁴CO₂ from [¹⁴C]benzene was analyzed after an incubation period of 3 weeks as described previously (36).

Growth of strain Seminole on benzoates and phenolics. Degradation of benzoate, phenol, 4-HBA, CAT, PCA, GA, PAA, and hexadecane, was studied in 250-ml Erlenmeyer flasks containing 100 ml of MSM supplemented with 2 M NaCl and filter-sterilized individual aromatic compounds incubated separately at 30°C without shaking under aerobic conditions. Degradation was monitored as depletion of the added compound using a UV spectrophotometer by scanning over specific wavelengths ranging between 200 and 400 nm. Growth was measured by estimation of total protein by the Lowry method (35).

Genome sequencing and assembly. The detailed procedure for the sample preparations was described previously (37). DNA was sheared to the size of ~2 kbp using nebulization at 30 lb/in² and -20°C for 2.5 min as described previously (38). Smaller fragments were removed using SPRI beads (catalog no. 000130) (39). DNA fragments were then end repaired (polished) by treating them with DNA polymerase and T4 polynucleotide kinase as described previously (37). Adaptors were then ligated using DNA ligase and end repaired using DNA polymerase. Single-stranded DNA molecules were then captured using DNA capture beads, emulsion PCR was performed as described previously (37), and the resulting amplified products were then run on 454 GS20 according to the recommendation of the manufacturer. Flows from the 454 system were assembled using Newbler, the 454 assembly software. Three different trimming lengths were used from the 454 system to reduce the number of artificial contigs produced due to poor qualities at the end of the contigs. The results were then utilized for assembly using Phrap.

Genomic analysis of hydrocarbon degradation potential. The genome was uploaded to the Integral Microbial Genomes (IMG) server (<http://img.jgi.doe.gov>) of the Joint Genome Institute for genome predictions, comparisons, and analysis. The clusters of orthologous groups (COGs) of protein sequences from strain Seminole were analyzed using the function category tool of the IMG. A one-sample *t* test was used to evaluate the statistically significant differences of gene abundances in each COG category between strain Seminole and other genomes of hydrocarbon-degrading halophiles deposited in the IMG bacterial genome database. A total of 10 genomes of hydrocarbon-degrading halophiles were used for comparative COG analysis.

The draft genome sequence of strain Seminole was screened for aromatic compound-degrading genes using a locally installed standalone BLAST software package (version 2.2.6). Genes encoding enzymes involved in various aromatic hydrocarbon degradation pathways that have been characterized in other organisms and deposited in the NCBI database were searched using BLASTp against the predicted peptides in the strain Seminole genome (27). The putative functions of the open reading frames (ORFs) predicted to be involved in aromatic compound degradation were confirmed by BLASTp search in the Uniprot database (40). The direction of transcription of the predicted genes and their relative positions on the contigs were determined by using GeneMark.hmm for Prokaryotes software (41).

Preparation of cell extracts. For proteomic studies, sufficient biomass was obtained by growing strain Seminole on lactate as described previously (42). Briefly, strain Seminole was grown on 5 mM lactate, fed twice as the sole source of carbon. At the end of the log growth phase, cells were centrifuged at 8,000 rpm for 15 min at 4°C, and the pellet was washed twice with sterile 0.14 M NaCl. The pellet was resuspended in MSM containing 2 M NaCl and used as an inoculum for the induction of enzymes involved in toluene, 4-HBA, or PAA degradation. Lactate-grown cells devoid of the respective hydrocarbon served as the control. Cells were harvested by centrifugation at 8,000 rpm for 15 min at 4°C. The cell pellets were washed once with 0.14 M NaCl and once with Tris-EDTA (TE) buffer (10 mM Tris-HCl, 1 mM EDTA [pH 8.0]). The pelleted cells were resuspended in TE buffer and disrupted using sonication (5 cycles of 15 s each). The protein concentration was determined by the Bradford method (43).

Proteomic analyses. Protein extracts were prefractionated on 12% SDS-PAGE gels and stained with Coomassie blue, and each lane was ex-

cised into 3 slices. Gel slices were destained by extensive washing with 50% acetonitrile–50 mM ammonium bicarbonate (pH 8), dehydrated with 100% acetonitrile, and dried briefly. Dried acrylamide pieces were rehydrated with 50 mM ammonium bicarbonate and reduced with Tris (2-carboxyethyl) phosphine hydrochloride for 1 h at room temperature. After incubation, the reducing buffer was replaced with 55 mM iodoacetamide in 50 mM ammonium bicarbonate, and samples were alkylated for 1 h at room temperature in the dark. Samples were then rinsed with ammonium bicarbonate, dehydrated with acetonitrile, and rehydrated/infiltrated with trypsin solution (8 µg trypsin per ml in 50 mM ammonium bicarbonate). After overnight digestion at 37°C, the trypsinolytic peptide products were extracted with 0.5% trifluoroacetic acid and analyzed by LC-MS/MS using an LTQ-OrbitrapXL mass spectrometer (ThermoFisher Scientific, MA) basically as described by Voruganti et al. (44) but with a 40-cm column packed with 3-µm Magic C₁₈ AQ particles (Bruker, MA). Proteins were identified by using Mascot (v2.2.2 from Matrix Science, Boston, MA) and a database generated by *in silico* digestion of the strain Seminole proteome predicted from the genome, as well as sequences for 114 common adventitious laboratory contaminants (<http://www.thegpm.org>). Peptide and protein identifications were validated using Scaffold (v4.0.6.1; Proteome Software, Inc., Portland, OR) using the ProteinProphet and PeptideProphet algorithms (45), with a minimum of 2 peptides identified and at protein thresholds that yielded a 1% false discovery rate for the data set. Proteins that contained similar peptides and could not be differentiated based on MS/MS analysis alone were grouped to satisfy the principles of parsimony. Differences in protein expression were analyzed by spectrum counting (46), comparing each protein's spectrum counts from extracts of cells cultured in lactate, toluene, 4-HBA, or PAA as indicated. Statistical significances in the total spectral counts were determined by Student's *t* test (2-tailed, equal variance) using a *P* value of <0.05 as the significance cutoff.

Nucleotide sequence accession numbers. The 16S rRNA gene sequence of *Arhodomonas* sp. clones obtained from this study have been deposited in the GenBank database under accession no. [KJ829488](https://doi.org/10.1093/nucleic-acids/gkz001) to [KJ829496](https://doi.org/10.1093/nucleic-acids/gkz002). The protein sequences of benzene-, toluene-, 4-HBA-, and PAA-degrading ORFs were deposited in the GenBank database under accession no. [JX311705](https://doi.org/10.1093/nucleic-acids/gkz003) to [JX311717](https://doi.org/10.1093/nucleic-acids/gkz004) and [KJ829497](https://doi.org/10.1093/nucleic-acids/gkz005) to [KJ829529](https://doi.org/10.1093/nucleic-acids/gkz006).

RESULTS AND DISCUSSION

Isolation and characterization of the benzene-degrading strain Seminole. Our understanding of the biology and genetic potential of halophilic and halotolerant microorganisms that degrade hydrocarbons in moderate- to high-salinity environments is severely lacking; consequently, we don't have the ability to use the natural potential of these organisms in the cleanup of contaminated hypersaline environments. Here, we describe the isolation and metabolic potential of a novel halophile, *Arhodomonas* sp. strain Seminole, which is capable of degrading benzene as the sole source of carbon and energy. Strain Seminole was isolated from a Sem-2 enrichment culture that was developed using soil obtained from an oil production facility in Oklahoma (23). The isolate is a Gram-negative, rod-shaped (0.5 by 2 to 3 µm in length), oxidase-positive, and catalase-negative bacterium. Figure 1 shows the phylogenetic relationship between strain Seminole and other halophiles according to their 16S rRNA gene sequences. A maximum likelihood tree was constructed using the 16S rRNA gene sequences of the members in *Gammaproteobacteria* that are halophilic or halotolerant and that degrade aromatic hydrocarbons. The strain formed a tight clade with *Arhodomonas* sp. strain Rozel, isolated in our laboratory from Rozel Point, UT (42), *Arhodomonas aquaeolei* strain HA-1 isolated from petroleum reservoir production fluid from Oklahoma (47), and *Arhodomonas recens* strain RS91, isolated from acidic brines of flotation enrichment from potassium

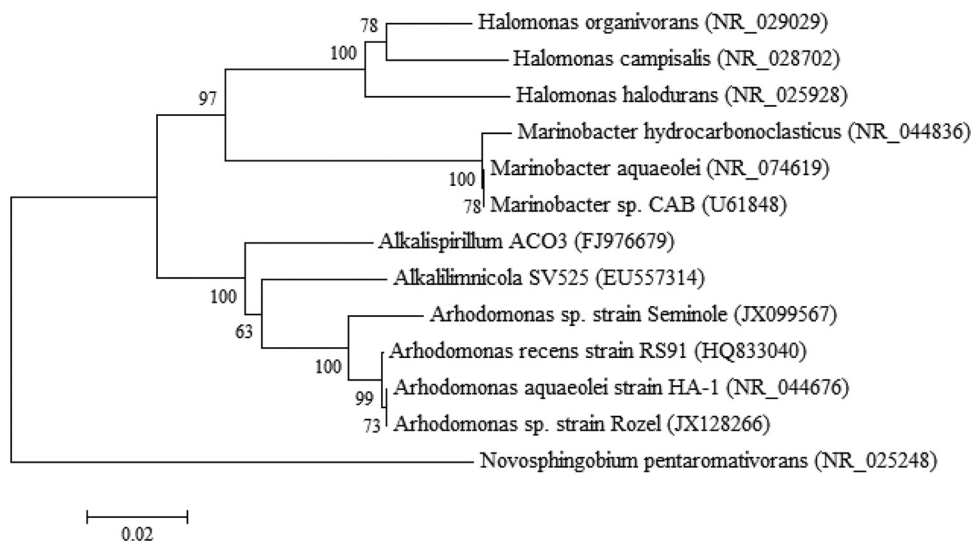


FIG 1 Phylogenetic tree using 16S rRNA gene sequences showing the relationship between strain Seminole and other halophilic/halotolerant bacteria. The tree was constructed by the maximum likelihood method and rooted with the 16S rRNA gene sequence of *Novosphingobium pentaromativorans*. Sequences for analysis were obtained from GenBank. Bootstrap values are shown next to the branches and were calculated as a percentage of 1,000 replicates. The size bar represents 2% sequence difference. Accession numbers of the bacteria are shown in parentheses.

minerals from Silvinit Co., Solikamsk, Russia (48). The strain shares 98, 97, and 96% sequence similarity, respectively, with *Arhodomonas* sp. strain Rozel, *Arhodomonas recens* strain RS91, and *Arhodomonas aquaeolei* strain HA-1. Furthermore, the strain also clustered with members of the genera in the *Alkalispirillum*-*Alkalilimnicola* group that are salt-tolerant haloalkaliphiles isolated from soda lake environments (49). In addition, analysis showed that *Arhodomonas* spp. formed a distinct cluster from that of other aromatic hydrocarbon-degrading halophiles/halotolerants belonging to *Gammaproteobacteria*, such as *Marinobacter* spp. and *Halomonas* spp.

In order to understand the diversity and adaptability of *Arhodomonas* spp. in different ecological niches, we analyzed soil, sediment, and water samples from both hydrocarbon-contaminated and uncontaminated sites with various levels of salinity (see Table S1 in the supplemental material). The presence of *Arhodomonas*

spp.-like organisms was confirmed by using *Arhodomonas*-specific primers, cloning, and sequencing of the PCR products. A phylogenetic tree using the 16S rRNA gene sequences of *Arhodomonas* spp. clones obtained in this study as well as sequences from the NCBI database was constructed. This limited survey revealed that the sequences formed two major clusters, despite their diverse habitats and geographic origin, each cluster harboring organisms from both hydrocarbon-contaminated as well as uncontaminated saline sites (see Table S1 and Fig. S1 in the supplemental material). Interestingly, *Arhodomonas* sp. strain 50B226 a3 (accession no. EU308280) from a Greek solar saltern did not cluster with other *Arhodomonas* spp. Also, *Arhodomonas* sp. strain SP71 (accession no. JF798749) from Santa Pola solar salterns and *Arhodomonas* sp. strain (accession no. KJ829495) from sediment from mangrove roots formed a distinct cluster. Since most of these organisms are not available in pure culture, determination of their ecophysiology and phylogenetic diversity cannot be fully interpreted.

Biodegradation of benzene and toluene by strain Seminole.

Strain Seminole was able to degrade 20 to 22 μmol of benzene in a period of 10 days in the presence of 2.5 M NaCl. The degradation of benzene was coupled to increased total cell protein, suggesting that strain Seminole was able to utilize benzene as the carbon and energy source (Fig. 2). The strain also degraded toluene, but no degradation of ethylbenzene or xylenes was observed (data not shown). In order to further evaluate the stoichiometry of benzene oxidation, separate experiments were carried out with [^{14}C]benzene. Evidence for mineralization of benzene by the strain was determined by measuring $^{14}\text{CO}_2$ from [^{14}C]benzene as described previously (36). Approximately 40 to 60% of the added [^{14}C]benzene was converted to $^{14}\text{CO}_2$ in a period of 3 weeks (data not shown), further suggesting utilization of benzene as the carbon source. The strain was also tested for its ability to degrade benzene at various salt concentrations ranging from 0 to 4 M NaCl. The strain was able to degrade 24 to 34 μmol of benzene within 2 to 3 weeks in bottles containing 1 to 2.5 M NaCl, with the maximum rate at 2 M NaCl (Fig. 3). Longer incubations (5 weeks) showed

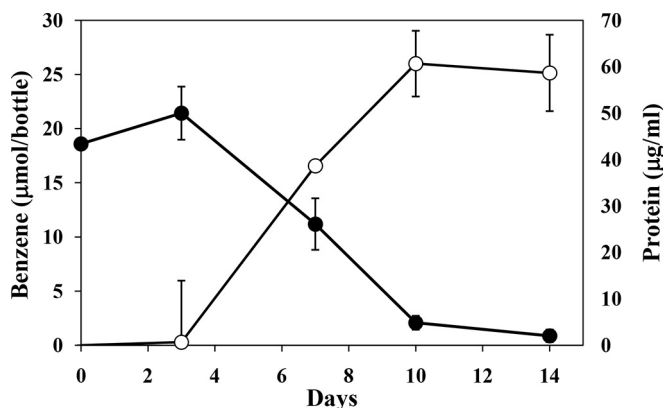


FIG 2 Biodegradation of benzene coupled to growth of *Arhodomonas* sp. strain Seminole in the presence of 2.5 M NaCl. Symbols: ●, benzene; ○, total cell protein. No degradation occurred in autoclaved control bottles. The data points are averages of triplicate bottles, and error bars indicate ± 1 standard deviation.

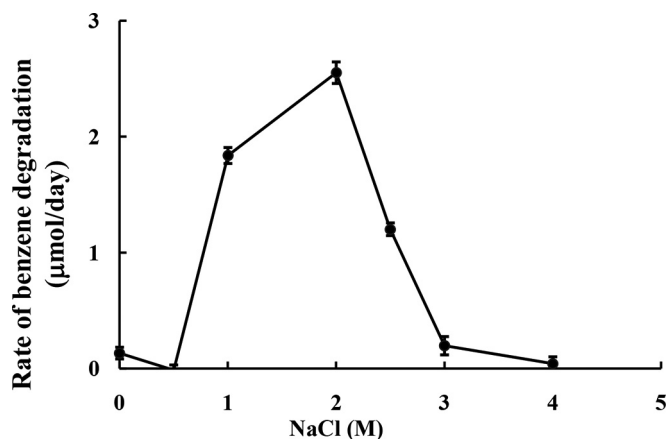


FIG 3 Rate of benzene degradation at different NaCl concentrations (●). Serum bottles containing 45 ml of MSM, 2 µl of neat benzene, and concentrations of NaCl ranging from 0 to 4 M were inoculated with 5 ml (~62 µg cell protein) of strain *Seminole*. Benzene was degraded at the maximum rate in the presence of 2 M NaCl, and no degradation was observed in the presence of 0, 0.5, and 4 M NaCl even after incubation for more than 4 weeks.

60% degradation of benzene in bottles containing 3 M NaCl. Benzene was not degraded at 4 M NaCl in 5 weeks (data not shown). Also, no benzene degradation was observed in bottles amended with 0 and 0.5 M NaCl, thus suggesting that the strain requires salt for growth; hence, it is a halophile. To further test the organism's halophilic nature on other substrates, we grew the organism on lactate as the sole carbon source in both the presence and absence of 2 M NaCl. The results showed that the organism grew on lactate only in the presence of 2 M NaCl, and no growth occurred in the bottles devoid of added salt, further suggesting that it is a true halophile (data not shown).

Biodegradation of benzoates and phenolics by strain *Seminole*. Strain *Seminole* was able to degrade phenol, 4-HBA, PCA, and PAA as the sole sources of carbon, as shown in Table 1. A lag period of 7 days was consistently observed when the organism was grown on 4-HBA, whereas no lag was observed when grown on PCA. The strain was able to grow on PAA, but only 45% disappearance of the substrate was observed over a period of 35 days of incubation. No growth was observed with benzoate, CAT, GA, and hexadecane even after 35 days of incubation. These results are consistent with the genome analysis. Although we detected ring-hydroxylating dioxygenases in the genome, no specific genes that code for enzymes catalyzing the initial step in the breakdown of benzoate, GA, and hexadecane pathways were detected. The organism's inability to grow on catechol is puzzling since this compound was predicted to be an intermediate in the benzene and toluene degradation pathway. We do not know the exact reason for this.

General genome features. The draft genome of strain *Seminole* has a single chromosome of 5,026,701 bp with a G+C content of 66.27%. The chromosome contains 5,180 predicted protein-coding genes (coding DNA sequences [CDS]) with an average size of 955 bp, giving a coding intensity of 86.87%. Analysis revealed 48 tRNA genes and 1 rRNA operon in the chromosome (see Table S2 in the supplemental material). Of the 5,180 CDS, 2,978 could be assigned to 22 different categories of clusters of orthologous groups (COGs) (see Table S3 and Fig. S2 in the supplemental material). Comparative analysis of the gene abun-

dances of each COG category between the genome of strain *Seminole* and the genomes of 10 other hydrocarbon-degrading halophiles in IMG (<http://img.jgi.doe.gov>) was evaluated using a one-sample *t* test. The abundances of genes related to amino acid transport and metabolism (11.34%), carbohydrate transport and metabolism (6.71%), and secondary metabolite biosynthesis, transport, and metabolism (4.17%) were significantly higher ($P < 0.05$) in the *Seminole* genome than the average abundances of 9.92%, 4.93%, and 3.25%, respectively, in the genomes of other 10 hydrocarbon-degrading halophiles (see Table S3). These results clearly suggest the organism's efficient carbohydrate and amino acid acquisition and metabolism for energy.

Genomic and proteomic elucidation of aromatic compound degradation pathways in strain *Seminole*. Analysis of the draft genome of strain *Seminole* predicted a number of catabolic ORFs encoding enzymes involved in the upper and lower degradation pathways of benzene, toluene, 4-HBA, and PAA. Most of these putative ORFs were found clustered together on the chromosome. BLASTp analysis of these ORFs against the UniProt database was performed to infer their catabolic functions (40). To further validate these predictions and identify the proteins involved in degradation pathways, we performed 1-dimensional (1-D) gel electrophoresis-based proteomic analysis (SDS-PAGE in combination with LC-MS/MS) of the cytosolic proteome of cells grown on lactate (control), toluene, 4-HBA, or PAA. Student's *t* test was used to determine whether the total spectral counts were significantly different between the lactate-grown and aromatic compound-grown proteomes.

(i) Degradation of benzene and toluene via the catechol ring cleavage pathway. Using the draft genome, we identified 19 ORFs (ORFs 1079 to 1097) arranged in a sequential fashion that code for proteins required for complete degradation of both benzene and toluene to acetaldehyde and pyruvate that can eventually enter the central metabolism (Table 2). The analysis showed that ORFs 1079 to 1084 encode a multicomponent phenol hydroxylase (PH)-like enzyme predicted to be involved in ring hydroxylation of benzene and toluene to form CAT and 3-methylcatechol, respectively. No genes homologous to those coding for benzene monooxygenases, benzene dioxygenases, toluene monooxygenases, and toluene dioxygenases that catalyze the initial ring oxidation steps were identified in the genome of strain *Seminole*, further

TABLE 1 Degradation of aromatic compounds by strain *Seminole*^a

Substrate	% degraded	Initial concn
Benzene	100	22–25 µmol/bottle
Toluene	100	22–25 µmol/bottle
Ethylbenzene	0	22–25 µmol/bottle
Xylene	0	22–25 µmol/bottle
Hexadecane	0	1%
Benzoate	0	2 mM
4-Hydroxybenzoic acid (4-HBA)	100	3 mM
Phenylacetic acid (PAA)	45	5.0 mM
Phenol	60	0.5 mM
Catechol (CAT)	0	0.5 mM
Protocatechuic acid (PCA)	100	2.5 mM
Gentisic acid (GA)	0	2.5 mM

^a Degradation of benzene, toluene, ethylbenzene, and xylenes was measured by GC. Degradation of benzoate, 4-HBA, PAA, phenol, CAT, PCA, and GA was measured by UV absorption at 228, 245, 257, 269, 274, 288, and 318 nm, respectively, using a UV-visible spectrophotometer.

TABLE 2 Genomic and proteomic identification of putative ORFs and proteins involved in the toluene degradation pathway in strain Seminole

ORF	Accession no. ^a	Putative function ^b	Avg spectral counts ^c		P value (Student's <i>t</i> test) ^d	Organism	% identity ^e	E value	UniProt accession no.
			Lactate	Toluene					
1079	JX311705	Phenol hydrolase assembly protein	0	0		<i>Acinetobacter nosocomialis</i> 28F	46	1e-09	U4Q6B8
1080	JX311706	Phenol hydrolase, β subunit	6	61	<0.00010	<i>Methylibium petroleiphilum</i>	52	e-102	A2SI51
1081	JX311707	Phenol hydroxylase component 2	0	1	0.37	<i>Ralstonia</i> sp. strain KN1	66	6e-25	Q9RAF7
1082	JX311708	Phenol hydroxylase component 3	6	60	<0.00010	<i>Wautersia numazuensis</i>	77	0	Q5KT19
1083	JX311709	Phenol hydroxylase component 4	0	5	0.00013	<i>Ralstonia</i> sp. strain E2	56	8e-35	O84962
1084	JX311710	Ferredoxin oxidoreductase	0	35	<0.00010	Uncultured bacterium	66	e-136	C6KUI9
1085	JX311712	Plant-type ferredoxin-like protein	0	0		<i>Azoarcus</i> sp. strain BH72	44	7e-15	A1K6K5
1086	JX311713	Catechol 2,3-dioxygenase	10	66	<0.00010	<i>Ralstonia metallidurans</i>	69	e-128	Q1LNR9
1087	JX311714	Uncharacterized protein	0	2	0.13	<i>Magnetospirillum</i> sp. strain SO-1	50	2e-39	M2ZC26
1088	JX311715	Transcriptional regulator	0	2	0.13	<i>Azoarcus</i> sp. strain BH72	48	9e-49	A1K899
1089	JX311716	Putative uncharacterized protein	0	0		<i>Thauera</i> sp. strain 63	59	9e-29	N6YI61
1090	JX311717	2-Hydroxyomuonic semialdehyde dehydrogenase	0	62	<0.00010	<i>Pseudomonas pseudoalcaligenes</i> CECT 5344	74	0	I7J281
1091	KJ829529	2-Hydroxyomuonic semialdehyde hydrolase	0	21	<0.00010	<i>Ralstonia metallidurans</i>	67	e-107	Q1LNT5
1092	KJ829528	2-Hydroxypenta-2,4-dienoate hydratase	2	26	0.00017	Uncultured bacterium	72	e-106	C6L0Y6
1093	KJ829527	Acetaldehyde dehydrogenase	6	44	0.00011	<i>Marinobacter algicola</i> DG893	76	e-122	A6EWL7
1094	KJ829526	4-Hydroxy-2-oxovalerate aldolase	1	59	<0.00010	<i>Cupriavidus necator</i> N-1	84	e-162	F8GQT8
1095	KJ829525	4-Oxalocrotonate decarboxylase	2	26	0.00037	<i>Thauera linaloolentis</i>	69	1e-92	N6XRY3
1096	KJ829524	Uncharacterized protein precursor	1	15	0.0011	<i>Alicyclophilus denitrificans</i>	42	2e-54	E8TUN5
1097	KJ829523	4-Oxalocrotonate tautomerase family enzyme precursor	0	0		<i>Pseudomonas</i> sp. strain GM18	60	1e-17	J2WLU6

^a Accession number assigned to each ORF in NCBI.

^b The putative functions of ORFs was predicted using BLASTp with the UniProt Knowledgebase (Swiss-Prot + TrEMBL) database. ORFs in boldface type were corroborated using LC-MS/MS analysis.

^c Average of total spectral counts obtained from SDS-PAGE gels run with lactate- or toluene-grown cell extracts from three bottles.

^d Student's *t* test was used to determine significant difference between total spectral counts of lactate-induced cells and toluene-induced cells obtained from Scaffold.

^e The percentage of identity was based on BLASTp hits against the UniProt Knowledgebase (Swiss-Prot + TrEMBL) database.

supporting our assertion that enzymes homologous to PH are responsible for the initial steps in benzene and toluene degradation in strain Seminole. ORFs 1086 to 1097, which were predicted to encode enzymes for *meta*-cleavage of CAT or the 3-methylcatechol degradation pathway, were found to be contiguous with the ORFs 1079 to 1084 (Fig. 4A; Table 2). A similar genetic organization of PH genes coupled with the CAT *meta*-cleavage pathway has been described in *Pseudomonas* sp. strain CF600 (50), *Comamonas testosteroni* TA441 (51), and *Cupriavidus necator* JMP134 (52).

In the case of benzene metabolism, ORF 1086 (2,3-CAT) catalyzes the ring fission of CAT to 2-hydroxyomuonic semialde-

hyde, and thus the formed ring cleavage product is further converted to 2-hydroxypent-2,4-dienoate by the activities of ORFs 1090, 1097, and 1095, which code for 2-hydroxyomuonic semialdehyde dehydrogenase, 4-oxalocrotonate tautomerase (4-oxalocrotonate isomerase), and 4-oxalocrotonate decarboxylase, respectively. In the next step, 2-hydroxypent-2,4-dienoate is hydroxylated to 4-hydroxy-2-oxovalerate by ORF 1092, which codes for 2-hydroxypenta-2,4-dienoate hydratase. Thus, formed 4-hydroxy-2-oxovalerate is split into acetaldehyde and pyruvate by ORF 1094, which codes for 4-hydroxy-2-oxovalerate aldolase. Acetaldehyde is converted to acetyl coenzyme A (acetyl-CoA) by ORF 1093, which codes for acetaldehyde dehydrogenase (Fig. 4B).

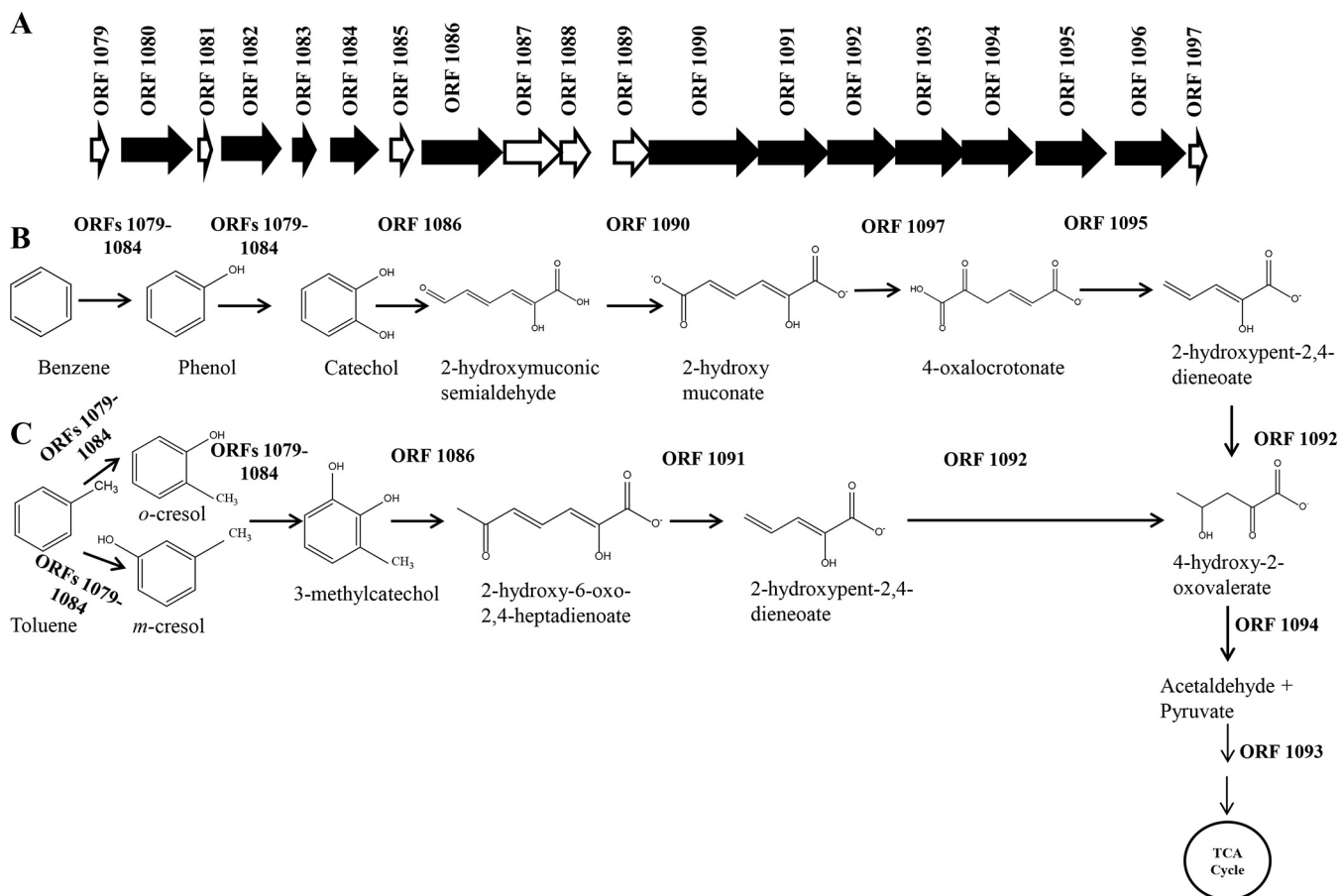


FIG 4 (A) Genetic organization of ORFs involved in degradation of benzene and toluene predicted in the genome of strain Seminole. The predicted ORFs are represented by arrows, and the arrowheads indicate the direction of their transcription. The gene sizes are not proportional to the arrows. ORFs represented by dark arrows were identified by LC-MS/MS in the toluene-grown cells. (B and C) Proposed benzene and toluene degradation pathways based on genomic and proteomic analyses. Putative functions of the ORFs are listed in Table 2. Multiple arrows indicate two or more steps.

Genomic analysis suggests that similar enzymes participate in the breakdown of toluene. For example, ORF 1086 catalyzes the ring cleavage of 3-methylcatechol to 2-hydroxy-6-oxo-2,4-heptadienoate. The thus-formed ring cleavage product is a ketone rather than an aldehyde, it cannot be further oxidized by the 2-hydroxy-6-oxo-2,4-heptadienoate dehydrogenase, and it is exclusively metabolized via the hydrolytic route (53). ORF 1091 codes for 2-hydroxy-6-oxo-2,4-heptadienoate hydrolase, which catalyzes the hydrolysis of 2-hydroxy-6-oxo-2,4-heptadienoate to 2-hydroxypent-2,4-dienoate, which is further converted to acetyl-CoA and pyruvate by steps identical to those in the benzene metabolism pathway (Fig. 4C).

Proteomic analysis was performed to corroborate the predicted ORFs. Of the predicted 19 ORFs involved in complete metabolism of toluene, we were able to identify 12 gene products that were significantly abundant ($P < 0.05$) in the proteome of toluene-induced cells compared to those in lactate-induced cells (Table 2). For example, four of the putative components of the PH complex, ORFs 1080, 1082, 1083, and 1084, were highly expressed, with average spectral counts of 61, 60, 5, and 35, respectively, in the proteome of toluene-grown cells. Based on these results, we predict that the PH catalyzes the oxidation of benzene and toluene

to corresponding 1-hydroxylated intermediates, such as phenol and *o*- or *m*-cresol, respectively, in the first step. Thus-formed phenol and *o*- or *m*-cresols are converted to CAT and 3-methylcatechol, respectively, in the second step of oxidation (Fig. 4B and C). Multicomponent PHs are soluble diiron monooxygenases that can hydroxylate a variety of aromatic compounds, including benzene, toluene, naphthalene, phenol, and methyl-substituted phenols (54).

Also identified in the proteome of toluene-grown cells was 2,3-CAT (ORF 1086), responsible for the *meta*-cleavage of 3-methylcatechol and other downstream enzymes responsible for the conversion of ring cleavage intermediates to central metabolites. These included 2-hydroxy-6-oxo-2,4-heptadienoate dehydrogenase (ORF 1090), 2-hydroxy-6-oxo-2,4-heptadienoate hydrolase (ORF 1091), 2-hydroxypent-2,4-dienoate hydratase (ORF 1092), acetaldehyde dehydrogenase (ORF 1093), 4-hydroxy-2-oxovalerate aldolase (ORF 1094), and 4-oxalocrotonate decarboxylase (ORF 1095). Analysis showed that some of the gene products were also detected in the lactate-grown cells but at significantly low levels (Table 2). The presence of low levels of these proteins could be due to the residual toluene in lactate-grown cells or could be induced

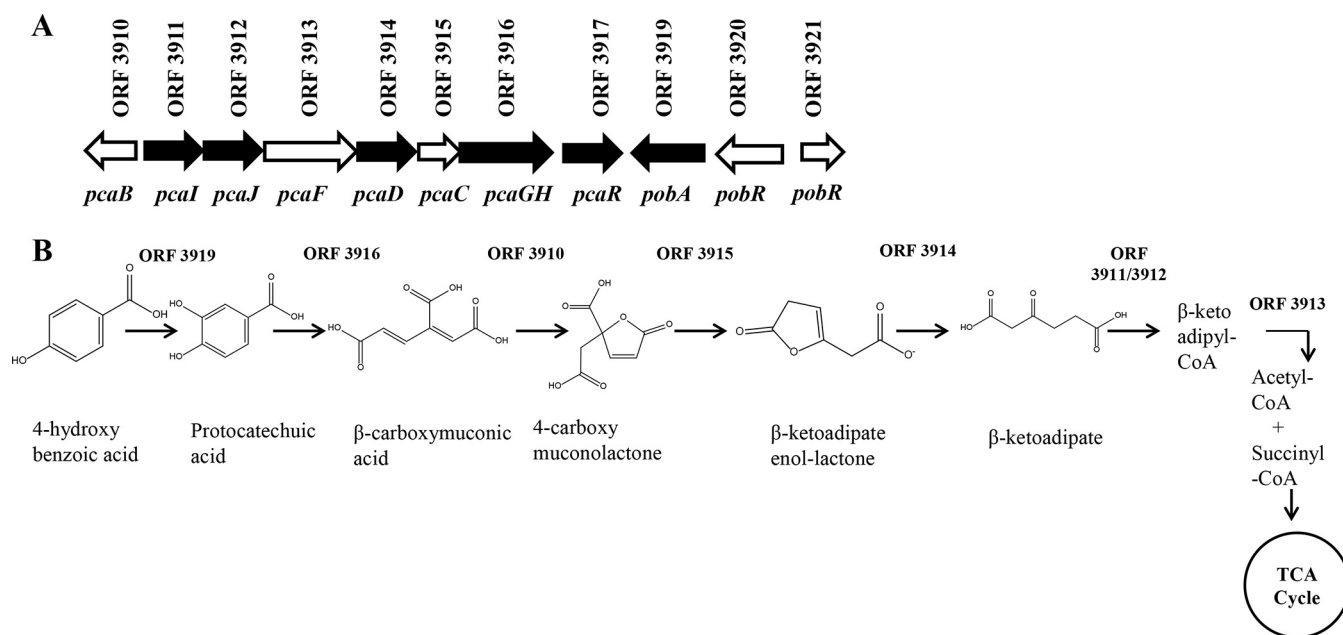


FIG 5 (A) Genetic organization of ORFs involved in degradation of 4-HBA predicted in the strain Seminole genome. The predicted ORFs are represented by arrows, and the arrowheads indicate the direction of their transcription. The ORFs represented by dark arrows were identified by proteomic analysis. The gene sizes are not proportional to the arrows. (B) Proposed 4-HBA degradation pathway based on genomic and proteomic analyses. Putative functions of the ORFs are listed in [Table 3](#).

by the presence of structurally similar metabolic intermediates of aromatic amino acids in the cells.

(ii) **4-Hydroxybenzoate degradation pathway via protocatechuate.** Strain Seminole was able to utilize 4-HBA as the sole source of carbon in the presence of 2 M NaCl. Genomic analysis revealed the presence of a complete set of genes (*pob* and *pca*) required for the 4-HBA degradation pathway, where 4-HBA is converted to PCA that undergoes *ortho*-ring cleavage and enters the β -ketoadipate pathway to form intermediates that will be assimilated via the TCA cycle ([Fig. 5](#)). Analysis showed that *pob* and *pca* genes are clustered together on a 21.6-kb contig of the genome. The *pob* genes were shown to encode the initial enzymes required for the 4-HBA degradation pathway, and the *pca* genes encode enzymes required for the downstream PCA branch of the β -ketoadipate pathway ([Fig. 5B](#)). The *pob* genes include *pobA* (ORF 3919), which encodes 4-hydroxybenzoate 3-monooxygenase, catalyzing the conversion of 4-HBA to PCA, and the *pobR* genes (ORF 3920 and 3921), which encode the AraC family transcriptional regulatory enzyme that activates the expression of the *pobA* gene in response to 4-HBA ([55](#)). The *pca* genes responsible for the conversion of PCA to β -ketoadipate included ORF 3916, which encodes α and β subunits of the 3,4-PCA (PcaGH) that catalyzes the conversion of PCA to β -carboxymuconic acid, which is transformed into 4-carboxymuconolactone by ORF 3910, encoding 3-carboxy-*cis*, *cis*-muconate cycloisomerase (PcaB). ORF 3915 codes for 4-carboxymuconolactone decarboxylase (PcaC), which converts 4-carboxymuconolactone into β -ketoadipate enol-lactone, which is then hydrolyzed by the product of ORF 3914, encoding 3-oxoadipate enol-lactonase (PcaD), into β -ketoadipate ([Fig. 5B](#)). ORFs 3911 and 3912 encode β -ketoadipyl succinyl-CoA transferase (PcaIJ), which catalyzes the conversion of β -ketoadipate to β -ketoadipyl-CoA. The cluster also includes

the *pcaF* gene, which codes for β -ketoadipyl CoA thiolase (ORF 3913), which catalyzes the last step transforming β -ketoadipyl-CoA to succinyl-CoA and acetyl-CoA ([56](#)), which can enter the TCA cycle. The *pcaR* gene (ORF 3917), which encodes the Icl-R type family transcriptional regulator required for inducible expression of *pcaBCDIJF* for conversion of β -carboxy-*cis*, *cis*-muconate to the TCA intermediates, was also clustered on the same contig ([56](#)).

Analysis of the cytosolic proteome of 4-HBA-grown cells has identified 6 key proteins involved in 4-HBA degradation pathway, substantiating the genome-predicted pathway ([Table 3](#)). These included 4-hydroxybenzoate 3-monooxygenase (ORF 3919), a homolog of *PobA* in *Chromohalobacter* sp. strain HS2 ([21](#)) that is responsible for the conversion of 4-HBA into PCA. The thus-formed PCA undergoes ring cleavage at the *ortho* position to form β -carboxymuconic acid and is catalyzed by 3,4-PCA encoded by ORF 3916. This is an important enzyme because PCA is a key intermediate produced from decaying lignin and other industrial aromatic compounds ([56](#)). Our proteomic analysis showed that a significant amount (average spectral count of 53) of ORF 3916 gene product was detected only in 4-HBA-grown cells compared to lactate-grown cells ([Table 3](#)). Also detected were 3-oxoadipate enol-lactonase (ORF 3914), β -ketoadipyl succinyl-CoA transferase A and B subunits (ORFs 3911 and 3912), and a regulatory protein (ORF 3917). All of these proteins were detected only in the 4-HBA-grown cells and not in the lactate-grown cells. The differences in spectral counts between the two samples were significantly different according to Student's *t* test ([Table 3](#)). These results clearly show the physiological and genetic ability of an extreme halophile to completely assimilate aromatic compounds originating from decaying plant material and environmental pollution in high-salinity environments. The genetic organizations of

TABLE 3 Genomic and proteomic identification of putative ORFs and proteins involved in the 4-HBA degradation pathway in strain Seminole

ORF	Accession no. ^a	Putative function ^b	Avg spectral counts ^c		P value (Student's <i>t</i> test) ^d	Organism	% identity ^e	E value	UniProt accession no.
			Lactate	4-HBA					
3910	KJ829514	3-Carboxy- <i>cis</i> , <i>cis</i> -muconate cycloisomerase	0	0		<i>Deinococcus geothermalis</i>	44	1e-8	Q1J3Z8
3911	KJ829513	β-Ketoadipyl succinyl-CoA transferase, subunit A	0	7	0.00081	<i>Azospirillum lipoferum</i> strain 4B	74	3e-176	G7ZFP6
3912	KJ829512	β-Ketoadipyl succinyl-CoA transferase, subunit B	0	5	0.0042	<i>Xanthomonas citri</i> pv. <i>mangiferaeindicae</i> LMG 941	69	5e-150	H8FEZ7
3913	KJ829511	β-Ketoadipyl CoA thiolase	0	0		<i>Marinobacter manganooxydans</i> Mn17-9	69	e-147	G6YUR0
3914	KJ829510	3-Oxoadipate enol-lactonase	0	5	0.00037	<i>Xanthobacter autotrophicus</i>	46	2e-59	A7IEC4
3915	KJ829509	4-Carboxymuconolactone decarboxylase	0	0		<i>Microvirga</i> sp. strain WSM3557	51	4e-27	I4Z0N1
3916	KJ829508	Protocatechuate 3,4-dioxygenase, α subunit	0	53	<0.0001	<i>Pseudomonas aeruginosa</i> 39016	52	e-119	E3A6W3
3917	KJ829507	Pca regulon regulatory protein	0	7	<0.0001	<i>Marinobacter</i> sp. strain ELB17	77	e-109	A3JCK5
3919	KJ829497	4-Hydroxybenzoate 3-monooxygenase	0	7	0.007	<i>Chromohalobacter</i> sp. strain HS2	82	0	A8I4C8
3920	KJ829498	AraC family of transcriptional regulator	0	0		<i>Halomonas</i> sp. strain A3H3	58	5e-91	T2L640
3921	KJ829506	Transcriptional regulator, AraC family (<i>pobR</i>)	0	0		<i>Halomonas elongata</i>	69	2e-34	E1V9E2

^a Accession number assigned to each ORF in NCBI.

^b The putative functions of ORFs was predicted using BLASTp with the UniProt Knowledgebase (Swiss-Prot + TrEMBL) database. ORFs in boldface type were corroborated using LC-MS/MS analysis.

^c Average of total spectral counts obtained from SDS-PAGE gels run with lactate- or 4-HBA-grown cell extracts from three flasks.

^d Student's *t* test was used to determine significant difference between total spectral counts of lactate-induced cells and toluene-induced cells obtained from Scaffold.

^e The percentage of identity was based on BLASTp hits against the UniProt Knowledgebase (Swiss-Prot + TrEMBL) database.

the upper pathway (*pob* genes) and lower pathway (*pca*) vary in different 4-HBA-degrading organisms. They are either found clustered together in a contiguous pattern or scattered over several portions of the genome. For example, the *pob* and *pca* genes were found clustered in two different locations in *Cupriavidus necator* JMP134 (52), were in three clusters in *Burkholderia xenovorans* LB400 (57), and were dispersed throughout the chromosome in *Polaromonas* sp. strain JS666 (58). However, in the Seminole genome, all of the genes needed for 4-HBA are located on one contig clustered together. Similar organization of *pob* and *pca* genes into one supraoperonic cluster was also reported in *Acinetobacter* sp. strain ADP1 (59).

(iii) Phenylacetate degradation pathway. Strain Seminole is also capable of degrading PAA as the sole source of carbon in the presence of 2 M NaCl. Our *in silico* analysis showed that the PAA catabolic pathway encodes protein in five putative functional units: (i) a substrate-activating protein, phenylacetyl-CoA ligase (PaaF), (ii) a ring hydroxylation complex (PaaGHIJK), (iii) a ring-opening protein (PaaN), (iv) a β-oxidation-like system (PaaACDE), and (v) two regulatory proteins (PaaX and PaaY) (60). Several investigators have used a different nomenclature to describe the *paa* genes, and in this article, we have adapted the system used by Luengo et al. (61). Analysis of the draft genome of Seminole revealed 15 ORFs putatively involved in complete PAA catabolism organized in distinct clusters on three different contigs (Fig. 6A). ORF 2986 encodes phenylacetyl-CoA ligase (PaaF),

which catalyzes the initial step of activation of PAA into phenylacetyl-CoA (PA-CoA) (62). PA-CoA is converted to ring 1,2-epoxyphenylacetyl-CoA by ORFs 2877 to 2881, which code for a ring oxygenase/reductase multicomponent complex (PaaK, PaaJ, PaaI, PaaH, and PaaG). ORFs 2877 to 2881 were found clustered together on contig 670 of the draft genome along with ORF 2883, which codes for a transcriptional regulator (PaaX) that controls the regulation of PAA degradative genes (Fig. 6A) (63). ORF 4130 codes for ring 1,2-epoxyphenylacetyl-CoA isomerase, which rearranges the epoxide ring 1,2-epoxyphenylacetyl-CoA into 2-oxepin-2-(3*H*)-ylideneacetyl CoA (oxepin-CoA). ORF 4128 (*paaN*) encodes a putative ring-opening enzyme that catalyzes the hydrolytic cleavage of the oxepin-CoA ring to form the intermediate, 3-oxo-5,6-dehydrosuberil-CoA (63). ORFs 4129, 4131, and 4133 (*paaA*, -C, and -E) code for enoyl-CoA hydratase, 3-hydroxybutyryl-CoA dehydrogenase, and β-ketoadipyl-CoA thiolase, respectively. These enzymes are similar to fatty acid β-oxidation enzymes and catalyze the β-oxidation of the ring-opened intermediate, leading to the formation of acetyl-CoA and succinyl-CoA, which enter the TCA cycle (Fig. 6B) (64). ORF 4133 encodes β-ketoadipyl thiolase (PaaE), which converts 3-oxo-5,6-dehydrosuberil-CoA to 2,3-dehydroadipyl-CoA, releasing an acetyl-CoA molecule (Fig. 6B). ORF 4129 encodes a putative hydratase that catalyzes the conversion of 2,3-dehydroadipyl-CoA into 3-hydroxyadipyl-CoA, which is further converted into β-ketoadipyl-CoA by ORF 4131 (*paaC*) encoding a 3-hydroxybutyryl-CoA de-

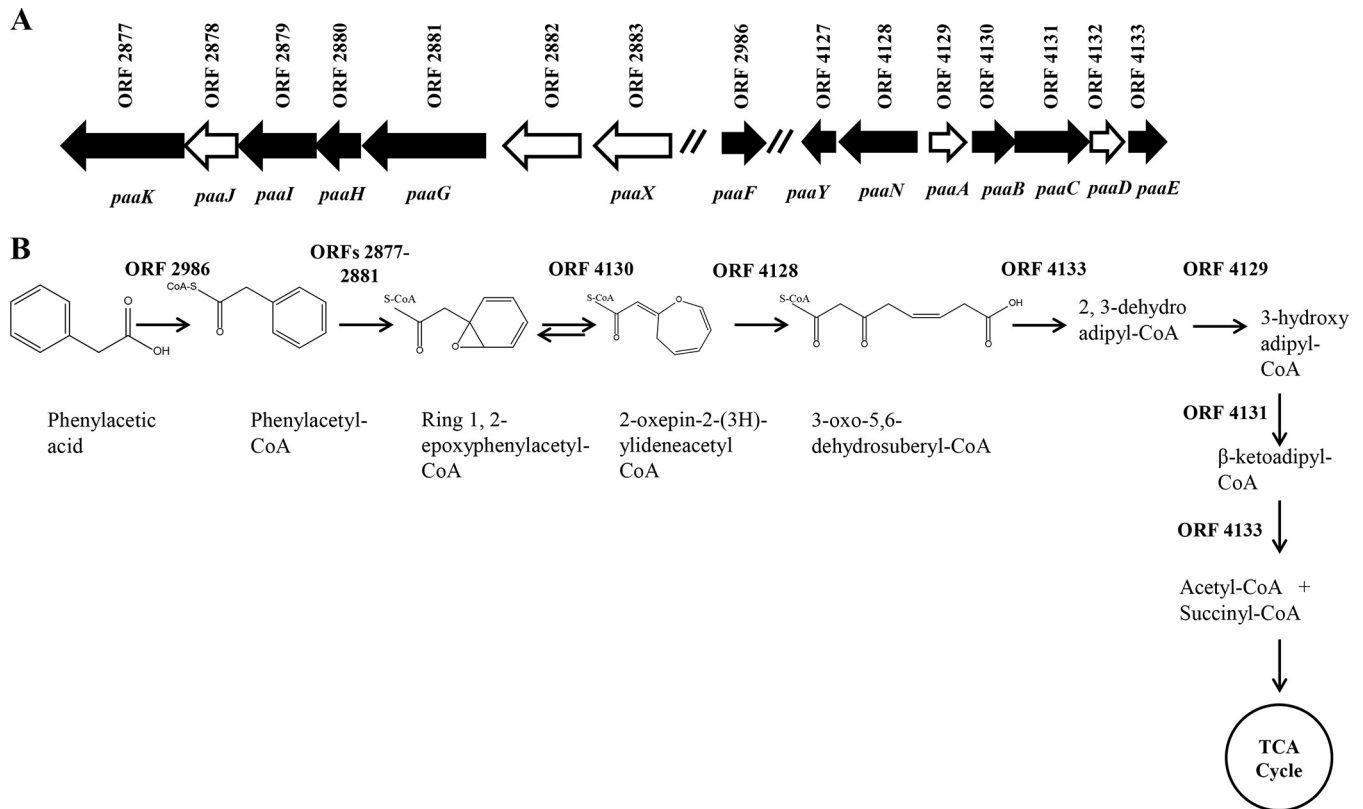


FIG 6 (A) Genetic organization of ORFs involved in degradation of PAA predicted in the strain Seminole genome. The predicted ORFs are represented by arrows, and the arrowheads indicate the direction of their transcription. ORFs represented by dark arrows were identified by proteomic analysis. The gene sizes are not proportional to the arrows. (B) Proposed PAA degradation pathway based on genomic and proteomic analyses. Putative functions of the ORFs are listed in Table 4. Multiple arrows indicate two or more steps.

hydrogenase that has 58% sequence identity to 3-hydroxyacyl-CoA dehydrogenase (65, 66). As in the previous step, ORF 4133 (β -ketoadipyl thiolase) thiolytically cleaves the β -ketoadipyl-CoA intermediate to produce acetyl-CoA and succinyl-CoA (64), which enters the TCA cycle. ORF 4127 (*paaY*), which encodes a regulatory protein, was also found clustered together with ORFs 4129 to 4133 (*paaAB-CDE*) on a 32,605-bp contig, 724 (Fig. 6A).

Of the 15 ORFs predicted bioinformatically, 10 proteins of the *paa* genes were more abundant in extracts of PAA-grown cells than in those of lactate-grown cells (Table 4). These included the *paaF*-encoded protein phenylacetyl-CoA ligase (ORF 2986) and *paaGHJK*-encoded proteins that are known to be the core subunits of the phenylacetyl-CoA epoxidase (ORFs 2881, 2880, 2879, and 2877). Also identified were PaaY, a putative regulator (ORF 4127), PaaN (ORF 4128), the ring-opening protein, PaaB (ORF 4130), the oxepin-CoA-forming protein, and PaaC and -E (ORFs 4131 and 4133), which are involved in the β -oxidation-like steps of PAA degradation (Table 4).

Our analysis shows that like many nonhalophiles, strain Seminole degrades PAA using an aerobic hybrid strategy that incorporates features of both aerobic and anaerobic degradation steps (61, 65). The first step is the CoA-dependent activation step (oxygen independent), in which PAA is converted to PA-CoA by a PA-CoA ligase (*PaaF*), and the thus-formed PA-CoA is transformed by a multicomponent oxygenase (aerobic step) into its ring 1,2-epoxide, which becomes an oxepin-CoA intermediate that undergoes

hydrolytic cleavage to form an aliphatic compound that is channeled through a β -oxidation-like mechanism to form acetyl-CoA and succinyl-CoA (66, 67). The *paa* genes are widely found in many phylogenetically unrelated bacteria (61). Our observations that PAA is degraded by a similar hybrid pathway in strain Seminole extends this mechanism to organisms living in high-salinity environments. *In silico* analysis shows that all 15 genes are arranged in clusters and distributed on three different contigs in the Seminole genome. Similar studies in nonhalophiles indicate that even though the arrangements of *paa* genes differ among different organisms, some features remain common to most described *paa* clusters (65). For example, genes encoding the ring-hydroxylating system (*PaaGHJK*) and β -oxidation system (*PaaACDE*) are usually clustered together in most *paa* systems, either at the same or different locations on the chromosome (65). A similar organization was also found to exist in the Seminole genome, where ORFs 2877 to 2881 (ring hydroxylating) and ORFs 4129 and 4131 to 4133 (β -oxidation system) are clustered on two different contigs (Fig. 6A).

The present work utilized a combination of genomic and proteomic approaches to elucidate degradation pathways for a variety of aromatic compounds at high salinity in a novel halophile, *Arhodomonas* sp. strain Seminole, isolated from a contaminated brine. *Arhodomonas* spp. are found to be widely distributed in contaminated as well as uncontaminated environments with various salinities, suggesting their important role in the natural atten-

TABLE 4 Genomic and proteomic identification of putative ORFs and proteins involved in PAA degradation pathway in strain Seminole

ORF	Accession no. ^a	Putative function ^b	Avg spectral counts ^c		P value (Student's <i>t</i> test) ^d	Organism	% identity ^e	E value	UniProt accession no.
			Lactate	PAA					
2877	KJ829522	Ring hydroxylation complex protein 4	0	25	<0.00010	<i>Nitrococcus mobilis</i> Nb-231	59	e-119	A4BNW0
2878	KJ829521	Phenylacetate-CoA oxygenase, PaaJ subunit	0	0		<i>Microvirga</i> sp. strain WSM3557	63	7e-54	I4YLN6
2879	KJ829520	Phenylacetate-CoA oxygenase	0	47	<0.00010	<i>Nitrococcus mobilis</i> Nb-231	65	2e-91	A4BNV8
2880	KJ829519	Phenylacetic acid degradation protein	0	7	0.002	<i>Nitrococcus mobilis</i> Nb-231	80	1e-40	A4BNV7
2881	KJ829518	Phenylacetate-CoA oxygenase, PaaG subunit	0	54	<0.00010	<i>Cupriavidus pinatubonensis</i>	75	e-144	Q46UU1
2882	KJ829517	Uncharacterized protein	0	0		<i>Pseudomonas</i> sp. strain HPB0071	48	2e-52	N2J7Q2
2883	KJ829516	PaaX family transcriptional regulator	0	4	0.12	<i>Alcanivorax dieselolei</i>	51	2e-86	K0CBT9
2986	KJ829515	Phenylacetate-CoA ligase	1	17	0.00035	<i>Herbaspirillum</i> sp. strain CF444	72	e-179	J2LFC3
4127	KJ829505	Phenylacetic acid degradation protein PaaY	0	10	<0.00010	<i>Thauera</i> sp. strain 28	71	5e-78	N6YDP9
4128	KJ829504	Phenylacetic acid degradation protein paaN2 (ring-opening enzyme)	0	21	<0.00010	<i>Nitrococcus mobilis</i> Nb-231	68	0	A4BNX0
4129	KJ829503	Putative enoyl-CoA hydratase I (<i>paaA2</i>)	0	0		<i>Pseudomonas</i> sp. strain Y2	59	3e-71	Q70IM9
4130	KJ829502	1,2-Epoxyphenylacetyl-CoA isomerase	0	5	0.00016	<i>Halomonas</i> sp. strain A3H3	61	4e-85	T2L8B6
4131	KJ829501	3-Hydroxybutyryl-CoA dehydrogenase	0	44	<0.00010	<i>Nitrococcus mobilis</i> Nb-231	61	e-174	A4BNX2
4132	KJ829500	Probable phenylacetic acid degradation protein	0	0		<i>Nitrococcus mobilis</i> Nb-231	67	3e-50	A4BNX3
4133	KJ829499	β-Ketoacyl-CoA thiolase	0	32	0.00035	<i>Azospirillum lipoferum</i> strain 4B	77	0	G7ZG05

^a Accession number assigned to each ORF in NCBI.

^b The putative functions of ORFs were predicted using BLASTp with the UniProt Knowledgebase (Swiss-Prot + TrEMBL) database. ORFs in boldface type were corroborated using LC-MS/MS analysis.

^c Average of total spectral counts obtained from SDS-PAGE gels ran with lactate or PAA-grown cell extracts from three flasks.

^d Student's *t* test was used to determine significant difference between total spectral counts of lactate-induced cells and PAA-induced cells obtained from Scaffold.

^e The percentage of identity was based on BLASTp hits against the UniProt Knowledgebase (Swiss-Prot + TrEMBL) database.

uation of petroleum compounds. Our data clearly demonstrate that the pathways and enzymes involved in the degradation of aromatic compounds in strain Seminole are similar to those described in nonhalophiles. Although halophilic proteins perform similar functions to their nonhalophilic homologs, they differ from their nonhalophilic homologs by maintaining stability and activity at high salinity. This is partly due to the low hydrophobicity of the protein core and the excess negative charge on the protein surface that is reflected in the low pI values of their proteins (68). A similar observation was made for some of the hydrocarbon-degrading proteins identified in strain Seminole (see Table S4 in the supplemental material). These proteins displayed relatively low pI values (theoretical) compared to their nonhalophilic homologs. Low pI is mostly due to high content of acidic residues like glutamate and aspartate on the surface of the proteins that forms a hydration shell to protect the enzyme from aggregation under high salinity (69, 70). These unique features enable halophilic proteins to function efficiently under extremely saline conditions, where nonhalophilic proteins lose their activity (69).

With the draft genome, we were able to predict putative steps

and requisite enzymes that catalyze degradation pathways of several aromatic compounds, including benzene, toluene, phenol, 4-HBA, PCA, and PAA. Furthermore, many of the predicted enzymes were identified using proteomic tools. It is important to point out that some of the predicted genes were not detected in the proteomic analysis. We surmise this could be due to low expression levels or the possibility that the genes were expressed at different times during the degradation process. We believe such an attempt to reconstruct metabolic steps using “-omics” tools represents a reliable platform for the development of strategies aimed at the exploitation of halophiles.

ACKNOWLEDGMENTS

This work was supported by funding from the Oklahoma Transportation Center (grant DTRT06-G-0014) and by the National Science Foundation (grant OCE1049301). We also thank the College of Arts and Sciences at Oklahoma State University for internal funding. Mass spectrometry analyses were performed in the DNA/Protein Resource Facility at Oklahoma State University, using resources supported by the NSF MRI and EPSCoR programs (award DBI/0722494).

We thank Janet Rogers from the DNA/Protein Resource Facility at Oklahoma State University for assistance with the LC-MS/MS analysis. We also thank Mostafa Elshahed for help with designing *Arhodomonas*-specific primers. We are grateful to Aharon Oren, Kathleen Duncan, Frank Loeffler, Mostafa Elshahed, Rene F. Bernier, and Eitan Ben-Dov for assistance in obtaining samples for the ecological distribution study.

REFERENCES

- Oren A, Gurevich P, Azachi M, Henis Y. 1992. Microbial degradation of pollutants at high salt concentrations. *Biodegradation* 3:387–398. <http://dx.doi.org/10.1007/BF00129095>.
- Margesin R, Schinner F. 2001. Biodegradation and bioremediation of hydrocarbons in extreme environments. *Appl. Microbiol. Biotechnol.* 56: 650–663. <http://dx.doi.org/10.1007/s002530100701>.
- Lefebvre O, Moletta R. 2006. Treatment of organic pollution in industrial saline wastewater: a literature review. *Water Res.* 40:3671–3682. <http://dx.doi.org/10.1016/j.watres.2006.08.027>.
- Whitehouse BG. 1984. The effects of temperature and salinity on the aqueous solubility of polynuclear aromatic hydrocarbons. *Mar. Chem.* 14:319–332. [http://dx.doi.org/10.1016/0304-4203\(84\)90028-8](http://dx.doi.org/10.1016/0304-4203(84)90028-8).
- Sorokin DY, Janssen AJH, Muyzer G. 2011. Biodegradation potential of halo(alkali)philic prokaryotes. *Crit. Rev. Environ. Sci. Technol.* 42:811–856. <http://dx.doi.org/10.1080/10643389.2010.534037>.
- Fathepure BZ. 2014. Recent studies in microbial degradation of petroleum hydrocarbons in hypersaline environments. *Front. Microbiol.* 5:173. <http://dx.doi.org/10.3389/fmicb.2014.00173>.
- Duran R. 2010. *Marinobacter*, p 1725–1735. In Timmis K (ed), *Handbook of hydrocarbon and lipid microbiology*. Springer, Berlin, Germany.
- Martins LF, Peixoto RS. 2012. Biodegradation of petroleum hydrocarbons in hypersaline environments. *Braz. J. Microbiol.* 43:865–872. <http://dx.doi.org/10.1590/S1517-83822012000300003>.
- Patzelt H. 2005. Hydrocarbon degradation under hypersaline conditions—some facts, some experiments and many open questions, p 105–122. In Gunde-Cimerman N, Oren A, Plemenitaš A (ed), *Adaptation to life at high salt concentrations in Archaea, Bacteria, and Eukarya*, vol 9. Springer, Dordrecht, Netherlands.
- Bertrand JC, Allmallah M, Acquaviva M, Mille G. 1990. Biodegradation of hydrocarbons by an extremely halophilic archaeobacterium. *Let. Appl. Microbiol.* 11:260–263. <http://dx.doi.org/10.1111/j.1472-765X.1990.tb00176.x>.
- Emerson D, Chauhan S, Oriol P, Breznak JA. 1994. *Haloferax* Sp D1227, a halophilic archaeon capable of growth on aromatic-compounds. *Arch. Microbiol.* 161:445–452. <http://dx.doi.org/10.1007/BF00307764>.
- Al-Mailem DM, Sorkhoh NA, Al-Awadhi H, Eliyas M, Radwan SS. 2010. Biodegradation of crude oil and pure hydrocarbons by extreme halophilic archaea from hypersaline coasts of the Arabian Gulf. *Extremophiles* 14:321–328. <http://dx.doi.org/10.1007/s00792-010-0312-9>.
- Tapilatu YH, Grossi V, Acquaviva M, Milton C, Bertrand JC, Cuny P. 2010. Isolation of hydrocarbon-degrading extremely halophilic archaea from an uncontaminated hypersaline pond (Camargue, France). *Extremophiles* 14:225–231. <http://dx.doi.org/10.1007/s00792-010-0301-z>.
- Fairley DJ, Boyd DR, Sharma ND, Allen CCR, Morgan P, Larkin MJ. 2002. Aerobic metabolism of 4-hydroxybenzoic acid in *Archaea* via an unusual pathway involving an intramolecular migration (NIH shift). *Appl. Environ. Microbiol.* 68:6246–6255. <http://dx.doi.org/10.1128/AEM.68.12.6246-6255.2002>.
- Cuadros-Orellana S, Pohlschröder M, Durrant LR. 2006. Isolation and characterization of halophilic archaea able to grow in aromatic compounds. *Int. Biodeterior Biodegrad.* 57:151–154. <http://dx.doi.org/10.1016/j.ibiod.2005.04.005>.
- Erdoğan Ş, Mutlu B, Korcan S, Güven K, Konuk M. 2013. Aromatic hydrocarbon degradation by halophilic archaea isolated from Çamaltı Saltern, Turkey. *Water Air Soil Pollut.* 224:1449. <http://dx.doi.org/10.1007/s11270-013-1449-9>.
- García MT, Ventosa A, Mellado E. 2005. Catabolic versatility of aromatic compound-degrading halophilic bacteria. *FEMS Microbiol. Ecol.* 54:97–109. <http://dx.doi.org/10.1016/j.femsec.2005.03.009>.
- Hinteregger C, Streichsieber F. 1997. *Halomonas* sp., a moderately halophilic strain, for biotreatment of saline phenolic waste-water. *Biotechnol. Lett.* 19:1099–1102. <http://dx.doi.org/10.1023/A:1018488410102>.
- Oie CSI, Albaugh CE, Peyton BM. 2007. Benzoate and salicylate degradation by *Halomonas campisalis*, an alkaliphilic and moderately halophilic microorganism. *Water Res.* 41:1235–1242. <http://dx.doi.org/10.1016/j.watres.2006.12.029>.
- Moreno MD, Sanchez-Porro C, Piubeli F, Frias L, Garcia MT, Mellado E. 2011. Cloning, characterization and analysis of cat and ben genes from the phenol degrading halophilic bacterium *Halomonas organivorans*. *PLoS One* 6:1. <http://dx.doi.org/10.1371/journal.pone.0021049>.
- Kim D, Kim SW, Choi KY, Lee JS, Kim E. 2008. Molecular cloning and functional characterization of the genes encoding benzoate and *p*-hydroxybenzoate degradation by the halophilic *Chromohalobacter* sp strain HS-2. *FEMS Microbiol. Lett.* 280:235–241. <http://dx.doi.org/10.1111/j.1574-6968.2008.01067.x>.
- Fairley DJ, Wang G, Rensing C, Pepper IL, Larkin MJ. 2006. Expression of gentisate 1,2-dioxygenase (*gdoA*) genes involved in aromatic degradation in two haloarchaeal genera. *Appl. Microbiol. Biotechnol.* 73:691–695. <http://dx.doi.org/10.1007/s00253-006-0509-0>.
- Nicholson CA, Fathepure BZ. 2004. Biodegradation of benzene by halophilic and halotolerant bacteria under aerobic conditions. *Appl. Environ. Microbiol.* 70:1222–1225. <http://dx.doi.org/10.1128/AEM.70.2.1222-1225.2004>.
- Lane DJ, Pace B, Olsen GJ, Stahl DA, Sogin ML, Pace NR. 1985. Rapid determination of 16S ribosomal RNA sequences for phylogenetic analyses. *Proc. Natl. Acad. Sci. U. S. A.* 82:6955–6959. <http://dx.doi.org/10.1073/pnas.82.20.6955>.
- Chang Y-J, Stephen JR, Richter AP, Venosa AD, Brüggemann J, Macnaughton SJ, Kowalchuk GA, Haines JR, Kline E, and White DC. 2000. Phylogenetic analysis of aerobic freshwater and marine enrichment cultures efficient in hydrocarbon degradation: effect of profiling method. *J. Microbiol. Methods* 40:19–31. [http://dx.doi.org/10.1016/S0167-7012\(99\)00134-7](http://dx.doi.org/10.1016/S0167-7012(99)00134-7).
- Fathepure BZ, Elango VK, Singh H, Bruner MA. 2005. Bioaugmentation potential of a vinyl chloride-assimilating *Mycobacterium* sp., isolated from a chloroethene-contaminated aquifer. *FEMS Microbiol. Lett.* 248:227–234. <http://dx.doi.org/10.1016/j.femsle.2005.05.033>.
- Altschul SF, Gish W, Miller W, Myers EW, Lipman DJ. 1990. Basic local alignment search tool. *J. Mol. Biol.* 215:403–410.
- Tamura K, Stecher G, Peterson D, Filipiński A, Kumar S. 2013. MEGA6: Molecular Evolutionary Genetics Analysis version 6.0. *Mol. Biol. Evol.* 30:2725–2729. <http://dx.doi.org/10.1093/molbev/mst197>.
- Ludwig W, Strunk O, Westram R, Richter L, Meier H, Yadukumar Buchner A, Lai T, Steppi S, Jobb G, Forster W, Brettske I, Gerber S, Ginhart AW, Gross O, Grumann S, Hermann S, Jost R, König A, Liss T, Lussmann R, May M, Nonhoff B, Reichel B, Strehlow R, Stamatakis A, Stuckmann N, Vilbig A, Lenke M, Ludwig T, Bode A, Schleifer KH. 2004. ARB: a software environment for sequence data. *Nucleic Acids Res.* 32:1363–1371. <http://dx.doi.org/10.1093/nar/gkh293>.
- Cole JR, Wang Q, Fish JA, Chai B, McGarrell DM, Sun Y, Brown CT, Porras-Alfaro A, Kuske CR, Tiedje JM. 2014. Ribosomal Database Project: data and tools for high throughput rRNA analysis. *Nucleic Acids Res.* 42:D633–D642. <http://dx.doi.org/10.1093/nar/gkt1244>.
- Sublette KL MA, Ford L, Duncan K, Thoma G, Brokaw J. 2005. Remediation of a spill of crude oil and brine without gypsum. *Environ. Geosci.* 12:115–125. <http://dx.doi.org/10.1306/eg.11160404040>.
- Youssef NH, Ashlock-Savage KN, Elshahed MS. 2012. Phylogenetic diversities and community structure of members of the extremely halophilic *Archaea* (order *Halobacteriales*) in multiple saline sediment habitats. *Appl. Environ. Microbiol.* 78:1332–1344. <http://dx.doi.org/10.1128/AEM.07420-11>.
- Ben-Dov E, Kushmaro A, Brenner A. 2009. Long-term surveillance of sulfate-reducing bacteria in highly saline industrial wastewater evaporation ponds. *Saline Syst.* 5:1–5. <http://dx.doi.org/10.1186/1746-1448-5-2>.
- Stackebrandt E, Goodfellow M. 1991. Nucleic acid techniques in bacterial systematics. *Modern microbiological methods*. Wiley, Chichester, United Kingdom.
- Lowry OH, Rosebrough NJ, Farr AL, Randall RJ. 1951. Protein measurement with the Folin phenol reagent. *J. Biol. Chem.* 193:265–275.
- Nicholson CA, Fathepure BZ. 2005. Aerobic biodegradation of benzene and toluene under hypersaline conditions at the Great Salt Plains, Oklahoma. *FEMS Microbiol. Lett.* 245:257–262. <http://dx.doi.org/10.1016/j.femsle.2005.03.014>.
- Margulies M, Egholm M, Altman WE, Attiya S, Bader JS, Bemben LA, Berka J, Braverman MS, Chen YJ, Chen Z, Dewell SB, Du L, Fierro JM, Gomes XV, Godwin BC, He W, Helgesen S, Ho CH, Irzyk GP, Jando SC, Alenquer ML, Jarvie TP, Jiracek KB, Kim JB, Knight JR, Lanza JR,

- Leamon JH, Lefkowitz SM, Lei M, Li J, Lohman KL, Lu H, Makhijani VB, McDade KE, McKenna MP, Myers EW, Nickerson E, Nobile JR, Plant R, Puc BP, Ronan MT, Roth GT, Sarkis GJ, Simons JF, Simpson JW, Srinivasan M, Tartaro KR, Tomasz A, Vogt KA, Volkmer GA, Wang SH, Wang Y, Weiner MP, Yu P, Begley RF, Rothberg JM. 2005. Genome sequencing in microfabricated high-density picolitre reactors. *Nature* 437:376–380. <http://dx.doi.org/10.1038/nature03959>.
38. Bodenteich A, Chissoe SL, Wang YF, Roe BA. 1993. Shotgun cloning as the strategy of choice to generate templates for high-throughput dideoxy-nucleotide sequencing, p 42–50. *In* Adams MD, Fields C, Venter JC (ed), Automated DNA sequencing and analysis techniques. Academic Press, London, United Kingdom.
39. DeAngelis MM, Wang DG, Hawkins TL. 1995. Solid-phase reversible immobilization for the isolation of PCR products. *Nucleic Acids Res.* 23: 4742–4743. <http://dx.doi.org/10.1093/nar/23.22.4742>.
40. UniProt Consortium. 2012. Reorganizing the protein space at the Universal Protein Resource (UniProt). *Nucleic Acids Res.* 40:D71–D75. <http://dx.doi.org/10.1093/nar/gkr981>.
41. Lukashin AV, Borodovsky M. 1998. GeneMark.hmm: new solutions for gene finding. *Nucleic Acids Res.* 26:1107–1115. <http://dx.doi.org/10.1093/nar/26.4.1107>.
42. Dalvi S, Azetsu S, Patrauchan MA, Aktas DF, Fathepure BZ. 2012. Proteogenomic elucidation of the initial steps in the benzene degradation pathway of a novel halophile, *Arhodomonas* sp. strain Rozel, isolated from a hypersaline environment. *Appl. Environ. Microbiol.* 78:7309–7316. <http://dx.doi.org/10.1128/AEM.01327-12>.
43. Bradford MM. 1976. A rapid and sensitive method for the quantitation of microgram quantities of protein utilizing the principle of protein-dye binding. *Anal. Biochem.* 72:248–254. [http://dx.doi.org/10.1016/0003-2697\(76\)90527-3](http://dx.doi.org/10.1016/0003-2697(76)90527-3).
44. Voruganti S, LaCroix JC, Rogers CN, Rogers J, Matts RL, Hartson SD. 2013. The anticancer drug AUY922 generates a proteomics fingerprint that is highly conserved among structurally diverse Hsp90 inhibitors. *J. Proteome Res.* 12:3697–3706. <http://dx.doi.org/10.1021/pr400321x>.
45. Keller A, Nesvizhskii AI, Kolker E, Aebersold R. 2002. Empirical statistical model to estimate the accuracy of peptide identifications made by MS/MS and database search. *Anal. Chem.* 74:5383–5392. <http://dx.doi.org/10.1021/ac025747h>.
46. Lundgren DH, Hwang S-I, Wu L, Han DK. 2010. Role of spectral counting in quantitative proteomics. *Expert Rev. Proteomics* 7:39–53. <http://dx.doi.org/10.1586/epr.09.69>.
47. Adkins JP, Madigan MT, Mandelco L, Woese CR, Tanner RS. 1993. *Arhodomonas aquaeolei* gen. nov., sp. nov., an aerobic, halophilic bacterium isolated from a subterranean brine. *Int. J. Syst. Bacteriol.* 43:514–520. <http://dx.doi.org/10.1099/00207713-43-3-514>.
48. Saralov AI, Kuznetsov BB, Reutskikh EM, Baslerov RV, Panteleva AN, Suzina NE. 2012. *Arhodomonas recens* sp. nov., a halophilic alkane-utilizing hydrogen-oxidizing bacterium from the brines of flotation enrichment of potassium minerals. *Microbiology* 81:630–637. <http://dx.doi.org/10.1134/S0026261712050062>.
49. Sorokin DY, Tourova TP, Kovaleva OL, Kuenen JG, Muyzer G. 2010. Aerobic carboxydrotrophy under extremely haloalkaline conditions in *Alkalispirillum/Alkalilimnicola* strains isolated from soda lakes. *Microbiology* 156:819–827. <http://dx.doi.org/10.1099/mic.0.033712-0>.
50. Shingler V, Franklin FC, Tsuda M, Holroyd D, Bagdasarjan M. 1989. Molecular analysis of a plasmid-encoded phenol hydroxylase from *Pseudomonas* CF600. *J. Gen. Microbiol.* 135:1083–1092.
51. Arai H, Ohishi T, Chang MY, Kudo T. 2000. Arrangement and regulation of the genes for meta-pathway enzymes required for degradation of phenol in *Comamonas testosteroni* TA441. *Microbiology* 146:1707–1715.
52. Perez-Pantoja D, De la Iglesia R, Pieper DH, Gonzalez B. 2008. Metabolic reconstruction of aromatic compounds degradation from the genome of the amazing pollutant-degrading bacterium *Cupriavidus necator* JMP134. *FEMS Microbiol. Rev.* 32:736–794. <http://dx.doi.org/10.1111/j.1574-6976.2008.00122.x>.
53. Powlowski J, Shingler V. 1994. Genetics and biochemistry of phenol degradation by *Pseudomonas* sp. CF600. *Biodegradation* 5:219–236. <http://dx.doi.org/10.1007/BF00696461>.
54. Leahy JG, Batchelor PJ, Morcomb SM. 2003. Evolution of the soluble diiron monooxygenases. *FEMS Microbiol. Rev.* 27:449–479. [http://dx.doi.org/10.1016/S0168-6445\(03\)00023-8](http://dx.doi.org/10.1016/S0168-6445(03)00023-8).
55. DiMarco AA, Ornston LN. 1994. Regulation of *p*-hydroxybenzoate hydroxylase synthesis by Pobr bound to an operator in *Acinetobacter calcoaceticus*. *J. Bacteriol.* 176:4277–4284.
56. Harwood CS, Parales RE. 1996. The beta-ketoadipate pathway and the biology of self-identity. *Annu. Rev. Microbiol.* 50:553–590. <http://dx.doi.org/10.1146/annurev.micro.50.1.553>.
57. Perez-Pantoja D, Donoso R, Agullo L, Cordova M, Seeger M, Pieper DH, Gonzalez B. 2012. Genomic analysis of the potential for aromatic compounds biodegradation in *Burkholderiales*. *Environ. Microbiol.* 14: 1091–1117. <http://dx.doi.org/10.1111/j.1462-2920.2011.02613.x>.
58. Mattes TE, Alexander AK, Richardson PM, Munk AC, Han CS, Stothard P, Coleman NV. 2008. The genome of *Polaromonas* sp. strain JS666: insights into the evolution of a hydrocarbon- and xenobiotic-degrading bacterium and features of relevance to biotechnology. *Appl. Environ. Microbiol.* 74:6405–6416. <http://dx.doi.org/10.1128/AEM.00197-08>.
59. Dal S, Trautwein G, Gerischer U. 2005. Transcriptional organization of genes for protocatechuate and quinate degradation from *Acinetobacter* sp. strain ADP1. *Appl. Environ. Microbiol.* 71:1025–1034. <http://dx.doi.org/10.1128/AEM.71.2.1025-1034.2005>.
60. Olivera ER, Minambres B, Garcia B, Muniz C, Moreno MA, Ferrandez A, Diaz E, Garcia JL, Luengo JM. 1998. Molecular characterization of the phenylacetic acid catabolic pathway in *Pseudomonas putida* U: the phenylacetyl-CoA catabolon. *Proc. Natl. Acad. Sci. U. S. A.* 95:6419–6424. <http://dx.doi.org/10.1073/pnas.95.11.6419>.
61. Luengo JM, Garcia JL, Olivera ER. 2001. The phenylacetyl-CoA catabolon: a complex catabolic unit with broad biotechnological applications. *Mol. Microbiol.* 39:1434–1442. <http://dx.doi.org/10.1046/j.1365-2958.2001.02344.x>.
62. Ferrandez A, Minambres B, Garcia B, Olivera ER, Luengo JM, Garcia JL, Diaz E. 1998. Catabolism of phenylacetic acid in *Escherichia coli*. Characterization of a new aerobic hybrid pathway. *J. Biol. Chem.* 273: 25974–25986.
63. Ferrandez A, Garcia JL, Diaz E. 2000. Transcriptional regulation of the divergent paa catabolic operons for phenylacetic acid degradation in *Escherichia coli*. *J. Biol. Chem.* 275:12214–12222. <http://dx.doi.org/10.1074/jbc.275.16.12214>.
64. Ismail W, El-Said Mohamed M, Wanner BL, Datsenko KA, Eisenreich W, Rohdich F, Bacher A, Fuchs G. 2003. Functional genomics by NMR spectroscopy. Phenylacetate catabolism in *Escherichia coli*. *Eur. J. Biochem.* 270:3047–3054. <http://dx.doi.org/10.1046/j.1432-1033.2003.03683.x>.
65. Navarro-Llorens JM, Patrauchan MA, Stewart GR, Davies JE, Eltis LD, Mohn WW. 2005. Phenylacetate catabolism in *Rhodococcus* sp. strain RHA1: a central pathway for degradation of aromatic compounds. *J. Bacteriol.* 187:4497–4504. <http://dx.doi.org/10.1128/JB.187.13.4497-4504.2005>.
66. Teufel R, Mascaraque V, Ismail W, Voss M, Perera J, Eisenreich W, Haehnel W, Fuchs G. 2010. Bacterial phenylalanine and phenylacetate catabolic pathway revealed. *Proc. Natl. Acad. Sci. U. S. A.* 107:14390–14395. <http://dx.doi.org/10.1073/pnas.1005399107>.
67. Fuchs G, Boll M, Heider J. 2011. Microbial degradation of aromatic compounds—from one strategy to four. *Nat. Rev. Microbiol.* 9:803–816. <http://dx.doi.org/10.1038/nrmicro2652>.
68. Fukuchi S, Yoshimune K, Wakayama M, Moriguchi M, Nishikawa K. 2003. Unique amino acid composition of proteins in halophilic bacteria. *J. Mol. Biol.* 327:347–357. [http://dx.doi.org/10.1016/S0022-2836\(03\)00150-5](http://dx.doi.org/10.1016/S0022-2836(03)00150-5).
69. Mevareh M, Frolow F, Gloss LM. 2000. Halophilic enzymes: proteins with a grain of salt. *Biophys. Chem.* 86:155–164. [http://dx.doi.org/10.1016/S0301-4622\(00\)00126-5](http://dx.doi.org/10.1016/S0301-4622(00)00126-5).
70. Reed CJ, Lewis H, Trejo E, Winston V, Evilia C. 2013. Protein adaptations in archaeal extremophiles. *Archaea* 2013:373275. <http://dx.doi.org/10.1155/2013/373275>.